

# STUDY AND IMPLEMENTATION OF AN EKF GIB-BASED UNDERWATER POSITIONING SYSTEM

A. Alcocer<sup>1</sup> P. Oliveira A. Pascoal

*Institute for Systems and Robotics and  
Department of Electrical Engineering,  
Instituto Superior Técnico,  
Av. Rovisco Pais, 1096 Lisboa Codex, Portugal  
e-mail: {alexblau,pjcro,antonio}@isr.ist.utl.pt*

Abstract: The paper addresses the problem of estimating the position of an underwater target in real time. In the scenario adopted, the target carries a pinger that emits acoustic signals periodically, as determined by a very high precision clock that is synchronized with GPS, prior to system deployment. The target is tracked from the surface by using a system of four buoys equipped with hydrophones. The buoys measure the times of arrival of the acoustic signals emitted by the pinger or, equivalently, the four target-to-buoy range measurements (so-called GIB system). Due to the finite speed of propagation of sound in water, these measurements are obtained with different latencies. The paper tackles the problem of underwater target tracking in the framework of Extended Kalman Filtering by relying on a purely kinematic model of the target. The paper further shows how the differently delayed measurements can be merged using a *back and forward* fusion approach. A measurement validation procedure is introduced to deal with dropouts and outliers. Simulation as well as experimental results illustrate the performance of the filter proposed. *Copyright ©2004 IFAC.*

Keywords: Underwater Vehicles, Navigation Systems, Extended Kalman Filters

## 1. INTRODUCTION

The last decade has witnessed the emergence of Ocean Robotics as a major field of research. Remotely Operated Vehicles (ROVs) and, more recently, Autonomous Underwater Vehicles (AUVs) have shown to be extremely important instruments in the study and exploration of the oceans. Free from the constraints of an umbilical cable,

AUVs are steadily becoming the tool *par excellence* to acquire marine data on an unprecedented scale and, in the future, to carry out interventions in undersea structures. Central to the operation of these vehicles is the availability of accurate vehicle navigation and/or positioning systems. The fact that electromagnetic signals do not penetrate below the sea surface makes the GPS unsuitable for underwater positioning. Hence, alternative solutions must be sought. The good propagation characteristics of sound waves in water makes acoustic positioning a viable solution.

Classical approaches to underwater vehicle positioning include Long Baseline (LBL) and Short

---

<sup>1</sup> Work supported in part by the Portuguese FCT POSI Programme under framework QCA III and by projects DREAM and MAROV of the FCT and MAYA of the AdI. The work of the first author was supported by an EC research grant in the scope of the FREESUB European Research Training Network.

Baseline (SBL) systems, to name but a few. See (Leonard *et al.*, 1998),(Larsen, 2001) and the references therein for an introduction to this challenging area. More recently, a number of methods have been proposed to "reproduce" the idea of GPS in the underwater environment. In (Youngberg, 1992) an underwater GPS concept was introduced. The system consists of surface buoys equipped with DGPS receptors that broadcast satellite information underwater, via acoustic telemetry. The underwater platform receives these messages from the buoys and computes its own position locally. Due to the technical difficulties inherent to acoustic communications, this concept has not yet materialized, as far as the authors are aware, in the form of a commercial product.

A different, yet related approach to acoustic underwater positioning has actually been implemented and is available commercially: the so-called GPS Intelligent Buoy (GIB) system (Thomas, 1998),(ACSA, 1999). This system consists of four surface buoys equipped with DGPS receivers and submerged hydrophones. Each of the hydrophones receives the acoustic impulses emitted periodically by a synchronized pinger installed on-board the underwater platform and records their times of arrival. As explained later in Section 6, the depth of the target is also available from the GIB system by coding that info in the acoustic emission pattern. The buoys communicate via radio with a central station (typically on-board a support vessel) where the position of the underwater target is computed. Due to the fact that position estimates are only available at the central station, this system is naturally suited for tracking applications.

Motivated by the latter approach to acoustic positioning, this paper addresses the general problem of estimating the position of an underwater target given a set of range measurements from the target to known buoy locations. Classically, this problem has been solved by resorting to triangulation techniques (Henry, 1978), which require that at least three range measurements be available at the end of each acoustic emission-reception cycle. This is hardly feasible in practice, due to unavoidable communication and sensor failures. It is therefore of interest to develop an estimator structure capable of dealing with the case where the number of range measurements available is time-varying. The paper shows how this problem can be tackled in the framework of Extended Kalman Filtering (EKF) whereby four vehicle-to-buoy range measurements drive a filter that relies on a simple kinematic model of the underwater target.

It is important to recall that due to the finite speed of propagation of sound in water, the range measurements are obtained at the buoys with

different latencies. To overcome this problem, the paper shows how the differently delayed measurements can be merged in an EKF setting by incorporating a *back and forward* fusion approach. Simulation as well as experimental results illustrate the performance of the filter proposed.

The paper is organized as follows. Section 2 describes the problem of underwater target positioning and introduces the relevant process and measurement models. Based on the models derived, Section 3 computes the matrices that are essential to the mechanization of a solution to the positioning problem in terms of an Extended Kalman Filter (EKF). Section 4 shows how the EKF structure can be changed to accommodate latency in the measurements. Simulation and experimental results that illustrate the performance of the filter proposed are discussed in Sections 5 and 7, while Section 6 describes briefly the acoustic validation and initialization procedures that were implemented. Finally, Section 8 contains the main conclusions and describes challenging problems that warrant further research.

## 2. PROBLEM STATEMENT. FILTER DESIGN MODELS

Consider an earth fixed reference frame  $\{O\}:=\{X_0, Y_0, Z_0\}$  and four (possibly drifting) buoys at the sea surface with submerged hydrophones at positions  $(X_{hi}, Y_{hi}, Z_{hi})$ ;  $i = 1, \dots, 4$  as depicted in Figure 1. For simplicity of presentation, we restrict ourselves to the case where the target moves in a plane at a fixed known depth  $Z_p$ . Its position in the earth fixed frame is therefore given by vector  $(x(t), y(t), Z_p)$ . The problem considered in this paper can then be briefly be stated as follows: obtain estimates  $(\hat{x}(t), \hat{y}(t))$  of the target position based on information provided by the buoys, which compute the travel time of the acoustic signals emitted periodically by a pinger installed onboard the underwater platform. The solution derived can be easily extended to the case where the target undergoes motions in three dimensional space.

### 2.1 Target (process) model

In what follows we avoid writing explicitly the dynamical equations of the underwater target being tracked and rely on its kinematic equations of motion only. Thus, a general solution for target positioning is obtained that fits different kinds of moving bodies such as AUVs, ROVs, divers, or even marine mammals.

The following notation will be used in the sequel:  $V$  is the total velocity of the vehicle in  $\{O\}$ ,  $\psi$

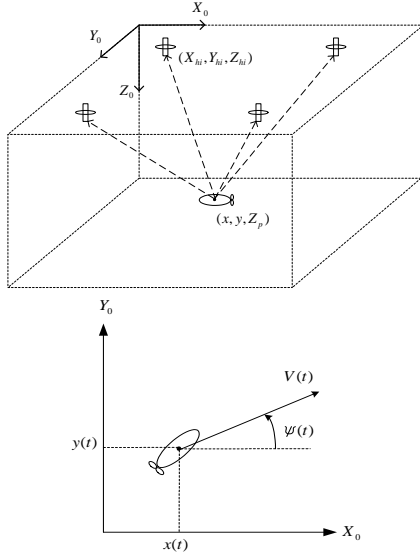


Fig. 1. Geometry of the target positioning problem.

denotes the angle between vector  $V$  and  $X_0$ , and  $r$  is the rate of variation of  $\psi$ . Notice that if the target moves in three dimensional space, and assuming the depth coordinated is known, tracking of its  $x, y$  coordinates can be done easily by re-interpreting  $V$  as the projection of the total velocity vector on its two first components. Given a continuous-time variable  $w(t)$ ,  $w(t_k)$  (abbv.  $w(k)$ ) denotes its values taken at discrete instants of time  $t_k = kh; k \in \mathbb{Z}_+$ , where  $h > 0$  denotes the sampling interval. Standard arguments lead to the discrete-time kinematic model for the target

$$\begin{cases} x(k+1) &= x(k) + hV(k) \cos \psi(k) \\ y(k+1) &= y(k) + hV(k) \sin \psi(k) \\ V(k+1) &= V(k) + \xi_v(k) \\ \psi(k+1) &= \psi(k) + hr(k) + \xi_\psi(k) \\ r(k+1) &= r(k) + \xi_r(k), \end{cases} \quad (1)$$

where the inclusion of the angular rate equation for  $r(k)$  captures the fact that the target undergoes motions in  $\psi$  that are not measured directly and are thus assumed to be unknown. The process noises  $\xi_v(k)$ ,  $\xi_\psi(k)$ , and  $\xi_r(k)$  are assumed to be stationary, independent, zero-mean, and Gaussian, with constant intensities  $\Xi_v$ ,  $\Xi_\psi$ , and  $\Xi_r$  respectively. The above model can be written as a Linear Parametrically Varying system of the form

$$\begin{aligned} \mathbf{x}(k+1) &= f(\mathbf{x}(k), \boldsymbol{\xi}(k)) \\ &= A(\mathbf{x}(k))\mathbf{x}(k) + L\boldsymbol{\xi}(k) \end{aligned} \quad (2)$$

where

$$A(\mathbf{x}(k)) = \begin{bmatrix} 1 & 0 & h \cos \psi(k) & 0 & 0 \\ 0 & 1 & h \sin \psi(k) & 0 & 0 \\ 0 & 0 & 1 & 0 & 0 \\ 0 & 0 & 0 & 1 & h \\ 0 & 0 & 0 & 0 & 1 \end{bmatrix}, \quad \mathbf{x}(k) = \begin{bmatrix} x(k) \\ y(k) \\ V(k) \\ \psi(k) \\ r(k) \end{bmatrix} \quad (3)$$

$$L = \begin{bmatrix} 0 & 0 & 0 \\ 0 & 0 & 0 \\ 1 & 0 & 0 \\ 0 & 1 & 0 \\ 0 & 0 & 1 \end{bmatrix}, \quad \boldsymbol{\xi}(k) = \begin{bmatrix} \xi_v(k) \\ \xi_\psi(k) \\ \xi_r(k) \end{bmatrix}. \quad (4)$$

## 2.2 Measurement model

In the set-up adopted for vehicle positioning the underwater pinger carries a high precision clock that is synchronized with those of the buoys (and thus with GPS) prior to target deployment. The pinger emits an acoustic signal every  $T$  seconds, at known instants of time. In each emission cycle, the pinger emits at discrete-time  $s$ , while buoys  $i; i = 1, \dots, 4$  compute their distances to the underwater unit at times  $r_i \geq s; r_i = N_i h$ , where  $N_i$  is the time it takes for the acoustic signal to reach buoy  $i$ , modulo the sampling interval  $h$ . Notice that the  $N_i$ 's are not necessarily ordered by increasing order of magnitude, since they depend on the distance of each of the buoys to the target. Notice also that even though  $z_i = z_i(s)$  refers to time  $s$ , its value can only be accessed at time  $r_i > s$ . It is therefore convenient to define  $\bar{z}_i(r_i) = z_i(r_i - N_i h) = z_i(s)$ , that is,  $\bar{z}_i(r_i)$  is the measurement of  $z_i(s)$  obtained at a later time  $r_i$ .

With the above notation, the noisy range measurements of each buoy are modeled as

$$z_i(s) = R_i(s) + [1 + \eta R_i(s)]\theta_i(s), \quad (5)$$

where

$$R_i^2(s) = (X_{hi} - x)^2 + (Y_{hi} - y)^2 + (Z_{hi} - Z_p)^2 \quad (6)$$

is the square of the distance from the vehicle to buoy  $i$  and  $x$  and  $y$  denote the horizontal position of the pinger at instant  $s$ . In the above,  $\theta_i(s)$  is a stationary, zero-mean, Gaussian white noise process with constant intensity  $\Theta_i$ . It is assumed that  $\theta_i(s)$  and  $\theta_j(s)$  are independent for  $i \neq j$ . The constant parameter  $\eta$  captures the fact that the measurement error increases as the range grows.

The full set of available measurements available over an interrogation cycle can vary from 0 to 4, depending on the conditions of the acoustic channel. Stated mathematically, the set of  $0 \leq m \leq 4$  measurements can be written as

$$\bar{\mathbf{z}}_r^m = \bar{\mathcal{C}}[\bar{z}_1(r_1), \dots, \bar{z}_4(r_4)]^T \quad (7)$$

where  $\bar{\mathcal{C}}: \mathcal{R}^4 \rightarrow \mathcal{R}^m$  denotes the operator that extracts and orders the  $m$  distances available

according to the time-sequence at which they are computed at the buoys. For reasons that will become clear later, it is important to define

$$\mathbf{z}^m(s) = \mathcal{C}[z_1(s), \dots, z_4(s)]^T \quad (8)$$

where  $\mathcal{C} : \mathcal{R}^4 \rightarrow \mathcal{R}^m$  denotes the operator that extracts the set of  $m$  distances available, as if they had been obtained at time  $s$ . In an analogous manner,  $\mathbf{z}^p(s)$ ;  $p \leq m$  will denote the first  $p$  components of  $\mathbf{z}^m(s)$ .

### 3. EXTENDED KALMAN FILTER DESIGN

In preparation for the development of a positioning system, and taking into account the relationship between  $\mathbf{z}^m(s)$  and  $\bar{\mathbf{z}}^m$ , consider an "ideal" situation where all or part of the  $m$  measurements obtained over an interrogation cycle are available at the corresponding interrogation time  $s$ , as condensed in vector  $\mathbf{z}^p(s)$ ;  $p \leq m$ . In this situation, given the nonlinear process and the observation models given by (1) and (5), respectively it is simple to derive an EKF structure to provide estimates of positions  $x(k)$  and  $y(k)$  based on measurements  $\mathbf{z}^p(s)$ , where  $s$  denotes an arbitrary interrogation time. The details are omitted; see for example (Anderson and Moore, 1979) or (Athans, 2003), and the references therein. Following standard practice, the derivation of an Extended Kalman Filter (EKF) for the above design model builds on the computation of the following Jacobian matrices about estimated values  $\hat{\mathbf{x}}(k)$  of the state vector  $\mathbf{x}(k)$ :

$$\hat{A}(\hat{\mathbf{x}}(k)) = \frac{\partial f(\mathbf{x}, \boldsymbol{\xi})}{\partial \mathbf{x}} \Big|_{\hat{\mathbf{x}}(k)}, \hat{L} = \frac{\partial f(\mathbf{x}, \boldsymbol{\xi})}{\partial \boldsymbol{\xi}} \Big|_{\hat{\mathbf{x}}(k)}, \quad (9)$$

$$\hat{C}(\hat{\mathbf{x}}(s)) = \frac{\partial \mathbf{z}^p}{\partial \mathbf{x}} \Big|_{\hat{\mathbf{x}}(s)}, \hat{D}(\hat{\mathbf{x}}(s)) = \frac{\partial \mathbf{z}^p}{\partial \boldsymbol{\theta}} \Big|_{\hat{\mathbf{x}}(s)} \quad (10)$$

It is straightforward to compute

$$\hat{A}(\hat{\mathbf{x}}(k)) = \begin{bmatrix} 1 & 0 & h \cos(\hat{\psi}(k)) & -h\hat{V}(k) \sin(\hat{\psi}(k)) & 0 \\ 0 & 1 & h \sin(\hat{\psi}(k)) & h\hat{V}(k) \cos(\hat{\psi}(k)) & 0 \\ 0 & 0 & 1 & 0 & 0 \\ 0 & 0 & 0 & 1 & h \\ 0 & 0 & 0 & 0 & 1 \end{bmatrix} \quad (11)$$

and

$$\hat{L} = \begin{bmatrix} 0 & 0 & 0 \\ 0 & 0 & 0 \\ 1 & 0 & 0 \\ 0 & 1 & 0 \\ 0 & 0 & 1 \end{bmatrix}. \quad (12)$$

Furthermore, by defining

$$\hat{C}_i(\hat{\mathbf{x}}(s)) = \begin{bmatrix} -\frac{X_{hi} - \hat{x}(s)}{\hat{R}_i(s)} & -\frac{Y_{hi} - \hat{y}(s)}{\hat{R}_i(s)} & 0 & 0 & 0 \end{bmatrix} \quad (13)$$

and

$$\hat{D}_i(\hat{\mathbf{x}}(s)) = 1 + \eta \hat{R}_i(s), \quad (14)$$

it follows that

$$\hat{C}(\hat{\mathbf{x}}(s)) = \text{stack}^p\{\hat{C}_j(\hat{\mathbf{x}}(s))\} \quad (15)$$

where  $\text{stack}^p$  denotes the operation of stacking  $p$  row matrices  $\hat{C}_j(\hat{\mathbf{x}}(s))$  by forcing the sequence of sub-indices  $j$  to match that in  $\mathbf{z}^p(s)$ . For example, if at time  $s$  we have access to the distances measured by buoys 1, 3, and 2 in this order, then

$$\hat{C}(\hat{\mathbf{x}}(s)) = \begin{bmatrix} C_1(\hat{\mathbf{x}}(s)) \\ C_3(\hat{\mathbf{x}}(s)) \\ C_2(\hat{\mathbf{x}}(s)) \end{bmatrix}. \quad (16)$$

$$(17)$$

Similarly,

$$\hat{D}(\hat{\mathbf{x}}(s)) = \text{diag}^p\{\hat{D}_i(\hat{\mathbf{x}}(s))\} \quad (18)$$

where the elements of the  $p \times p$  diagonal matrix  $\hat{D}(\hat{\mathbf{x}}(s))$  are ordered in an analogous manner. Note that the dimensions of  $\hat{C}$  and  $\hat{D}$  vary according to the number of measurements that we suppose are available at time  $s$ . With an obvious abuse of notation, the measurement noise intensity matrix can then be written as

$$\Theta(s) = \text{diag}^p\{\Theta_j(s)\} \quad (19)$$

where  $\Theta_j(s) = \text{E}\{\boldsymbol{\theta}_j^2(s)\}$ , while the process noise intensity matrix admits the representation

$$\Xi(k) = \text{E}\{\boldsymbol{\xi}(k)\boldsymbol{\xi}^T(k)\} = \begin{bmatrix} \Xi_v(k) & 0 & 0 \\ 0 & \Xi_r(k) & 0 \\ 0 & 0 & \Xi_\psi(k) \end{bmatrix}. \quad (20)$$

The matrices  $A(\hat{\mathbf{x}}(k))$  and  $\hat{A}(\hat{\mathbf{x}}(k))$  have an important property that will be used later:

*Property 1.* Given any nonzero positive integer  $N$ , define

$$\left\{ \begin{array}{l} \alpha_1 = \alpha_1(N, k) \triangleq \sum_{l=0}^N \cos(\hat{\psi}(k) + l\hat{r}(k)), \\ \alpha_2 = \alpha_2(N, k) \triangleq \sum_{l=0}^N \sin(\hat{\psi}(k) + l\hat{r}(k)), \\ \beta_1 = \beta_1(N, k) \triangleq \sum_{l=0}^N l \cos(\hat{\psi}(k) + l\hat{r}(k)), \\ \beta_2 = \beta_2(N, k) \triangleq \sum_{l=0}^N l \sin(\hat{\psi}(k) + l\hat{r}(k)) \end{array} \right. \quad (21)$$

Then it can be shown that

$$\hat{\Phi}(k + Nh, k) \triangleq \prod_{l=0}^N \hat{A}(\hat{\mathbf{x}}(k + lh)) = \quad (22)$$

$$\begin{bmatrix} 1 & 0 & h\alpha_1 & -h\hat{V}(k)\alpha_2 & -h\hat{V}(k)\beta_1 \\ 0 & 1 & h\alpha_2 & h\hat{V}(k)\alpha_1 & h\hat{V}(k)\beta_2 \\ 0 & 0 & 1 & 0 & 0 \\ 0 & 0 & 0 & 1 & hN \\ 0 & 0 & 0 & 0 & 1 \end{bmatrix} \quad (23)$$

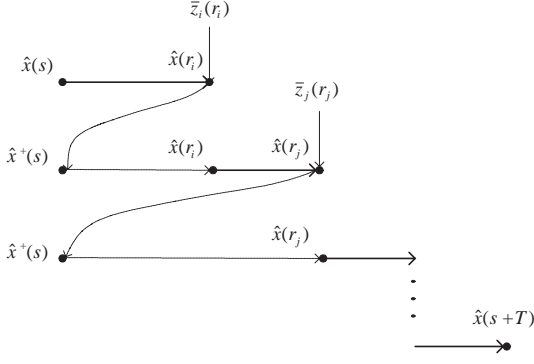


Fig. 2. *Back and forward* fusion approach. The solid line denotes the availability of real time output filter data. and

$$\Phi(k + Nh, k) \triangleq \prod_{l=0}^N A(\hat{\mathbf{x}}(k + lh)) = \quad (24)$$

$$\begin{bmatrix} 1 & 0 & h\alpha_1 & 0 & 0 \\ 0 & 1 & h\alpha_2 & 0 & 0 \\ 0 & 0 & 1 & 0 & 0 \\ 0 & 0 & 0 & 1 & hN \\ 0 & 0 & 0 & 0 & 1 \end{bmatrix}. \quad (25)$$

For  $N = 0$ ,

$$\hat{\Phi}(k, k) = \Phi(k, k) \triangleq I. \quad (26)$$

#### 4. FUSING DELAYED MEASUREMENTS WITH THE EKF

From the discussion above, the main problem to be overcome in the design on acoustic positioning system for the underwater unit is caused by the variable time-delay affecting each buoy measurement. The question then arises as to how delayed measurements can be naturally incorporated into an EKF structure. The reader will find in (Larsen *et al.*, 1998) a survey of different methods proposed in the literature to fuse delayed measurements in a linear Kalman Filter structure. In that work, a new method is also presented that relies on "extrapolating" the measurement of a variable obtained with latency to present time, using past and present estimates of the Kalman Filter. The problem tackled in this paper differs from that studied in (Larsen *et al.*, 1998) in two main aspects: the underlying estimation problem is nonlinear, and the components of the output vector at a given time  $s$  are accessible with different latencies. As shown below, this problem can be tackled using a *back and forward* fusion approach which recomputes the filter estimates every time a new measurement is available. This computational complexity involved is drastically reduced by resorting to Property 1.

In this work the estimator runs at a sampling period  $h$  typically much smaller than  $T$ , the interrogation period of the underwater pinger. Let

$s$  be an arbitrary instants of time at which the underwater pinger emits an acoustic signal and let  $i \leq m$  be the buoy that first receives this signal at time  $r_i = s + N_i h$ . Further let  $\bar{z}_i(r_i)$  be the corresponding distance. Up until time  $r_i$  no new measurements are available, and a pure state and covariance prediction update are performed using the EKF set-up described before, leading to the predictor (see (Anderson and Moore, 1979))

$$\hat{\mathbf{x}}(k + h) = A(\hat{\mathbf{x}}(k))\hat{\mathbf{x}}(k) \quad (27)$$

$$P(k + h) = \hat{A}(\hat{\mathbf{x}}(k))P(k)\hat{A}^T(\hat{\mathbf{x}}(k)) + \hat{L}\Xi\hat{L}^T \quad (28)$$

with  $k = s, s + h, \dots, r_i$ . Upon reception of the first measurement  $\bar{z}_i(r_i)$  available during the interrogation cycle, and assuming that the state  $\hat{\mathbf{x}}(k)$  and covariance  $P(k)$  estimates at time  $k = s$  have been stored, it is possible to go back to time  $s$  and perform a filter state and covariance update as if measurement  $\bar{z}_i(r_i)$  were available at  $s$ . Using the notation introduced before with  $p$  set to 1, this leads to

$$\hat{\mathbf{x}}^+(s) = \hat{\mathbf{x}}(s) + K(s)[z^1(s) - \hat{z}^1(s)] \quad (29)$$

$$P^+(s) = P(s) - P(s)\hat{C}^T$$

$$[\hat{C}P(s)\hat{C}^T + \hat{D}\Theta\hat{D}^T]^{-1}\hat{C}P(s) \quad (30)$$

$$K(s) = P^+(s)\hat{C}^T[\hat{D}\Theta\hat{D}^T]^{-1} \quad (31)$$

where  $\hat{z}^1(s)$  denotes the estimate of  $z^1(s)$ . A new prediction cycle can now be done moving forward in time until a new measurement  $\bar{z}_j$  is available, using (27)-(28) and starting with the updated states and covariance found in (29)-(30). Due to property 1, this prediction can be expressed in a computationally simple form. Let  $r_j = s + N_j h$  be the time step at which measurement  $\bar{z}_j(r_j)$  is received. Then, the prediction cycle from  $s$  to  $r_j$  can be computed in closed form as

$$\hat{\mathbf{x}}(r_j) = \Phi(r_j, s)\hat{\mathbf{x}}^+(s) \quad (32)$$

$$P(r_j) = \hat{\Phi}(r_j, s)P^+(s)\hat{\Phi}^T(r_j, s) + \sum_{l=0}^{N_j-1} \hat{\Phi}(s + lh, s)\hat{L}\Xi\hat{L}^T\hat{\Phi}^T(s + lh, s) \quad (33)$$

Again, upon computation of measurement  $\bar{z}_j(r_j)$  it is possible to go back to time  $s$  and perform a filter state and covariance update as if measurements  $\bar{z}_i(r_i)$  and  $\bar{z}_j(r_j)$  were available at  $s$ . This is done using equations (29)-(30), with the one-dimensional vector  $z^1(s)$  replaced by  $z^2(s)$  and matrices  $\hat{C}, \hat{D}$ , and  $\Theta$  matrices recomputed accordingly. This *back and forward* structure proceeds until the  $m$  measurements available over an interrogation cycle (starting at  $s$  and ending at  $s + T$ ) are dealt with. This procedure is then repeated for each interrogation cycle. The overall structure of the algorithm proposed is depicted in Figure 2.

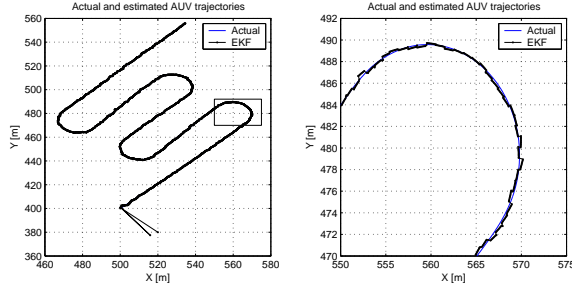


Fig. 3. Left: Actual and estimated simulated AUV trajectories. Right: idem, details of boxed area

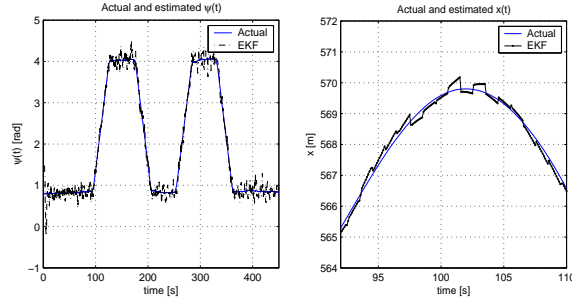


Fig. 4. Left: actual and estimated  $\psi(t)$ . Right: detail of actual and estimated  $x(t)$ .

## 5. SIMULATION SETUP AND RESULTS

In the simulations, four buoys were placed at the corners of a square with a 1Km side. The depth of the hydrophones  $Z_{hi}$  was set to 5m for all the buoys. A typical target trajectory was simulated at a nominal speed of 1m/s and a turning diameter of 15m. The target maneuvered in the horizontal plane, at a constant depth  $Z_p = 50$ m. The range measurements were generated every  $T = 1$ s and corrupted according to (5) with a 0.1m standard deviation Gaussian noise. The EKF was run at a sampling period of  $h = 0.1$ s. The actual and estimated initial states, as well as the process and measurement noise intensities, were set to

$x(0)$	$[500 \ 400 \ 1 \ \pi/4 \ 0]^T$
$\hat{x}_0$	$[520 \ 380 \ 0.5 \ \pi/2 \ 0]^T$
$P_0$	$\text{diag}\{(20)^2 \ (20)^2 \ (0.5)^2 \ (0.05)^2 \ (0.005)^2\}$
$\Xi_v$	$(0.001)^2$
$\Xi_\psi$	$(0.005)^2$
$\Xi_r$	$(0.02)^2$
$\Theta_i$	$(0.1)^2, \quad i = 1, \dots, 4$
$\eta$	0.001

Figure 3 shows a simulation of actual and estimated 2D target trajectories and the details of a turning maneuver. Figure 4 shows actual and estimated  $\psi(k)$  as well as the details of actual and estimated  $x(k)$ . Notice the 'jump' in the estimates whenever a new measurement is available. Notice also how the heading estimates change slowly in the course of a turning maneuver.

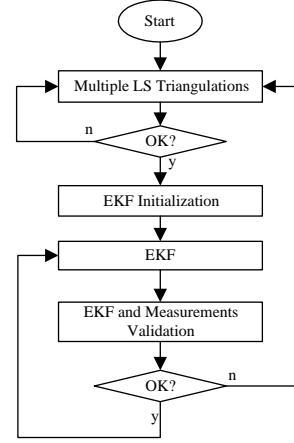


Fig. 5. Measurement validation and Initialization procedures.

## 6. MEASUREMENT VALIDATION AND EKF INITIALIZATION

In preparation for actual tests of the GIB-based system at sea, this section discusses practical issues that warrant careful consideration. As is well known, the implementation of any acoustic positioning system requires that mechanisms be developed to deal with dropouts and outliers that arise due to acoustic path screening, partial system failure, and multipath effects. See for example (Vaganay *et al.*, 1996) and the references therein for an introduction to this circle of ideas and for an interesting application to AUV positioning using a Long Baseline System. In the case of the GIB system, the problem is further complicated because of the mechanism that is used to transmit the depth of the target. In fact, the pinger onboard the vehicle emits two successive acoustic pulses during each emission cycle, the time delay between the two pulses being proportional to the pinger depth. Ideally, the data received at each buoy during each emission cycle consists of two successive pulses only. In practice, a number of pulses may be detected depending on the "quality" of the acoustic channel. For example, the data received may correspond to a number of situations that include the following: i) only the first pulse is received - a valid range measurement is acquired but the depth info is not updated, ii) only the second pulse is received - data contains erroneous information, and iii) a single pulse is received as a consequence of multipath effects - data may be discarded or taken into consideration if a model for multipath propagation is available.

In the present case, following the general strategy outlined in (Vaganay *et al.*, 1996), a two stage procedure was adopted that includes a time-domain as well as a spatial-domain validation. Time-domain validation is done naturally in an EKF setting by examining the residuals associated with the measurements (i.e., the difference

between predicted and measured values as they arrive), and discarding the measurements with residuals that exceed a certain threshold. During system initialization, or when the tracker is not driven by valid measurements over an extended period of time, a spatial-domain validation is performed to overcome the fact that the estimate of the target position may become highly inaccurate. This is done via an initialization algorithm that performs multiple Least Squares (LS) triangulations based on all possible scenarios compatible with the set of measurements received and selects the solution that produces the smallest residuals. Figure 6 shows raw and validated measurements for one of the GIB buoys. The vertical scale is presented in milliseconds to stress the fact that each of the buoys computes its distance to the pinger indirectly, by measuring the time-delay between the reception and the emission of the first acoustic pulse. Notice how the depth information is coded in the delay between two consecutive acoustic pulses. The figure on the right shows the boxed area in detail.

The diagram in Figure 5 depicts the procedure for measurement validation. In an initialization scenario, or whenever a filter reset occurs, the multiple triangulation algorithm is performed until a valid solution is obtained, that is, until the residuals of the resulting set of measurements are less than a certain threshold. Once a valid position fix is obtained, the EKF is initialized and a procedure that relies on the EKF estimates and *a priori* information about the vehicle’s maximum speed and noise characteristics selects the valid measurements. The EKF will be reset if the residuals become bigger than a threshold or if the duration of a pure prediction phase (that is, the time window during which no validated measurements are available) lasts too long.

## 7. EXPERIMENTAL SETUP AND RESULTS

Experimental data were recorded during tests at sea in Sines, Portugal, during the period from 23-24th April, 2003 using a commercially available GIB system. The data were processed off-line using the positioning algorithm described. Data validation was done using the methodology described in the previous section. Four buoys were moored in an approximate square configuration with a 500 meter side. The pinger was maneuvered at an approximate depth of 5 meters. In the data subset selected for post-processing, acoustic reception at hydrophones was good and four measurements were available most of the time. However, one of the buoys had reception problems and did not commute to Differential GPS mode. This situation was easily tackled in an EKF framework by giving

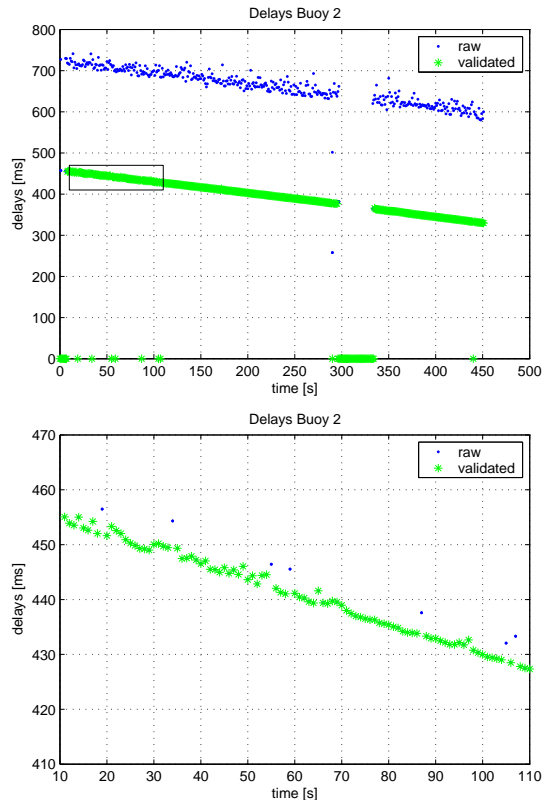


Fig. 6. Top: Raw and validated measurements from one of the buoys during tests at sea. Bottom: idem, detail of boxed area.

higher variance to the measurements provided by that buoy. The following conditions were adopted:

$P_0$	$\text{diag}\{(10)^2 (10)^2 (1)^2 (0.05)^2 (0.005)^2\}$
$\Xi_v$	$(0.01)^2$
$\Xi_\psi$	$(0.005)^2$
$\Xi_r$	$(0.025)^2$
$\Theta_i$	$(1)^2$ if DGPS, $(4)^2$ if GPS, $i = 1, \dots, 4$
$\eta$	0.001

Figure 7 shows the estimated target trajectories using EKF and a simple LS Triangulation. The EKF performs well, even with 1 or 2 measurements, whereas Triangulation is unable to compute solutions. As expected, Triangulation produces noisier estimates than the EKF solution. Figure 8 is a screenshot of the graphical interface used to report the status of the target tracking algorithm.

## 8. CONCLUSIONS AND FUTURE WORK

The paper proposed a solution to the problem of estimating the position of an underwater target in real time. The experimental set-up adopted consists of a system of four buoys that compute the times of arrival of the acoustic signals emitted periodically by a pinger installed on-board the moving platform (so-called GIB system). The positioning system fuses the vehicle-to-buoy range measurements by resorting to an

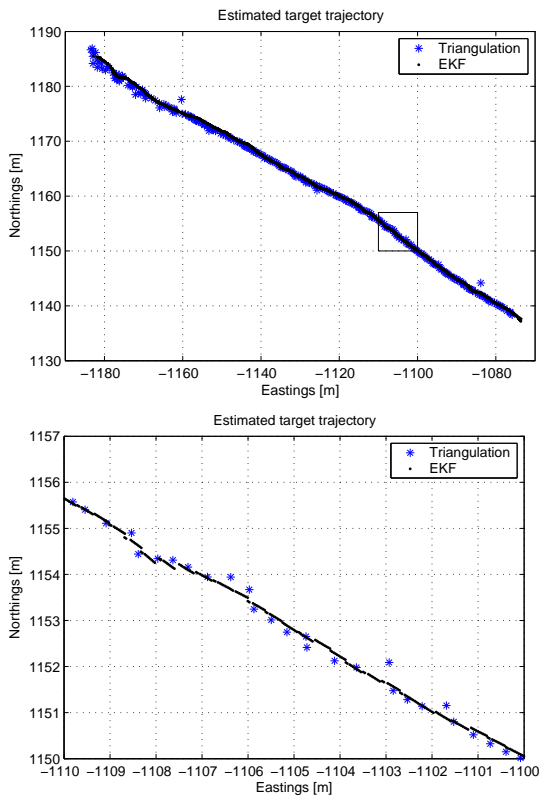


Fig. 7. Top: Estimated target trajectories with Triangulation and EKF based Estimator. Bottom: idem, zoom of boxed area.

Extended Kalman Filter (EKF)-structure that addresses explicitly the problems caused by measurement delays. By dealing directly with each buoy measurement as it becomes available, a system is obtained that exhibits far better performance than that achievable with classical triangulation schemes, where all buoy measurements are collected before an estimate of the target's position can be computed. Simulation as well as experimental results show that the proposed filter is computationally effective and yields good results, even in the presence of acoustic outliers or a reduced number of valid buoy measurements. Future work will include the study of different nonlinear filter structures for which convergence results can in principle be derived. Another interesting topic of research is how to fuse the filter estimates with other kinds of sensorial data.

#### REFERENCES

ACSA, ORCA (1999). *Trajectographe GIB Manuel Utilisateur*.

Anderson, B. D. O. and J. B. Moore (1979). *Optimal Filtering*. Prentice Hall.

Athans, Michael (2003). *Viewgraphs and Notes on Dynamic Stochastic Estimation, Filtering, Prediction and Smoothing*. ISR/IST, Lisbon, PT.

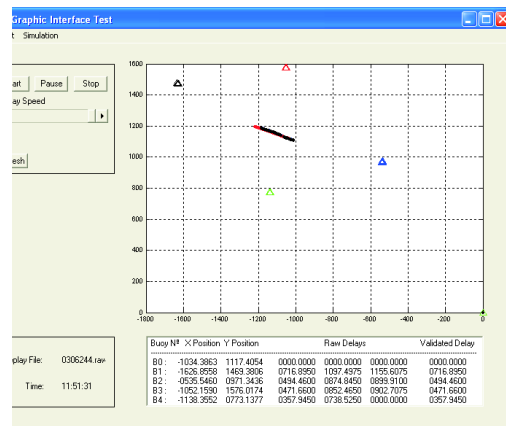


Fig. 8. Screenshot of tracking software interface.

Henry, T. D. (1978). Acoustic transponder navigation. In: *IEEE Position Location and Navigation Symp.*, pp. 237-244.

Larsen, Mikael Bliksted (2001). *Autonomous Navigation of Underwater Vehicles*. Ph.D. Dissertation. Department of Automation, Technical University of Denmark.

Larsen, T. D., N. K. Poulsen, N. A. Andersen and O. Ravn (1998). Incorporation of time delayed measurements in a discrete-time kalman filter. In: *Proceedings of the 37th Conference on Decision and Control, Tampa, Florida, USA*, pp. 3972-3977.

Leonard, J., A. Bennett, C. Smith and H. Feder (1998). *Autonomous underwater vehicle navigation*. MIT Marine Robotics Laboratory Technical Memorandum 98-1.

Thomas, H. G. (1998). Gib buoys: An interface between space and depths of the oceans. In: *Proceedings of IEEE Autonomous Underwater Vehicles, Cambridge, MA, USA*, pp. 181-184.

Vaganay, J., J. Leonard and J. Bellingham (1996). Outlier rejection for autonomous acoustic navigation. In: *Proceedings of IEEE International Conference on Robotics and Automation, Minneapolis, MN, USA*, pp. 2174-2181.

Youngberg, James W. (1992). Method for extending GPS to Underwater Applications. US Patent 5,119,341, June 2 1992.